

High-Temperature Decomposition of Fe- and Cr-Doped NiO Produced by a Novel Flame Spray Technique

Mark E. Duffield¹ · Gordon J. Tatlock¹ ·
John F. Lewis²

Received: 3 January 2017 / Published online: 24 February 2017

© The Author(s) 2017. This article is published with open access at Springerlink.com

Abstract A novel thick film technology has been developed for the manufacture of electric heating elements from partially oxidised Ni–Cr–Fe alloy powder. The sprayed films were a mixture of metallic alloys and Ni-based oxides. Electron microscopy and analysis were used to monitor the transformations in the films during subsequent heat treatment. In particular, it was found that homogeneous grains of Cr- and Fe-doped Ni-based oxides transformed into NiO grains containing numerous Ni-, Cr- and Fe-rich spinel particles with a typical size of 40 nm.

Keywords Doped NiO · Ni–Cr–Fe spinels · Thick film heating elements · Flame spraying

Introduction

A novel thick film technology has been developed for the manufacture of energy-efficient, electric heating elements. The two-step procedure makes use of existing flame spray technology to partially oxidise a powdered Ni–Cr–Fe alloy (approximately 75 wt% Ni, 15 wt% Cr, 10 wt% Fe) and subsequently deposit it upon an enamelled substrate. Due to a more efficient transfer of heat, these films can achieve the same performance (e.g. for cooking or drying) as traditional coiled wire

✉ Gordon J. Tatlock
g.j.tatlock@liverpool.ac.uk

Mark E. Duffield
eg0u61c5@student.liverpool.ac.uk

John F. Lewis
john@johnf-lewis.co.uk

¹ Centre for Materials and Structures, School of Engineering, University of Liverpool, Liverpool, UK

² 2DHeat Ltd., Dashmore Business Park, Lock Street, St Helens, Merseyside, UK

elements while operating at considerably lower temperatures. The associated energy savings make the thick film heating elements a potentially interesting alternative for any manufacturer employing current coiled wire technology.

During the initial flame spray oxidation, individual powder particles receive different levels of heat exposure due to their differing flight paths through the flame. Consequently, the particles experience varying degrees of oxidation. The range of different phases exhibited in the resultant powder is reflected in the inhomogeneous nature of the thick film deposit. In order to derive a better understanding of the electrical conduction mechanisms and pathways operating at the atomic level, and the variation in positive temperature coefficient with progressive use, a combination of optical, chemical and electrical characterisation techniques has been used to examine the material at different stages of manufacture. In particular, since the oxidation of the alloy powder involves high-temperature exposure followed by rapid cooling, the thick film heating elements contain a collection of metastable phases, and their transformations during reheating are examined in this paper.

Experimental Procedures

Starting Material

The raw material, from which the doped NiO is formed, is a nitrogen gas-atomised Ni–Cr–Fe alloy produced from ingots of Inconel 600 (one of the families of austenitic Ni–Cr-based superalloys [1]). The specific composition of the powder, determined via X-ray fluorescence (XRF) by manufacturer ECKA granules, is presented in Table 1. The concentrations of Si and Mn are elevated above those in the original alloy due to their introduction as fluxing agents during the gas atomisation process.

Thick Film Manufacture

Oxidation of Powdered Alloy

In the first stage of manufacture, the nickel alloy powder, of typical diameter 34 μm , is partially oxidised by passing it through an oxyacetylene flame. During this process, a powder feed rate of approximately 8 g/min is maintained using a nitrogen carrier gas. In order to cool the high-temperature powder particles, the spray is directed into an aluminium quenching bath, filled with water to a depth of 120 mm. The degree of oxidation can be changed by adjusting the spray path length. In the

Table 1 Chemical composition of the powdered alloy

Element	Ni	Cr	Fe	Si	Cu	Mn	C
wt%	Bal.	14.9	8.6	0.55	0.3	0.13	0.06

current study, the Ni alloy powder was oxidised over a spray path length of 600 mm.

Deposition of Partially Oxidised Powder

The second stage of production involves the deposition of the partially oxidised ECKA 500 powder onto a substrate surface at a powder feed rate of approximately 2 g/min. During this process, the spray nozzle travels at 300 mm/s back and forth across the target material, advancing 5 mm forward at the end of each pass. As the deposit is concentrated within a 12-mm-diameter circle, there is considerable overlap between each successive deposition line. The aim of this overlap is to keep the element thickness as consistent as possible so that the resistance and, by extension, heat generation are as uniform as possible. Four such heating elements, positioned at 90° spacing and connected in a parallel circuit, are shown attached to an alumina pre-coated beam line vacuum vessel in Fig. 1. Each thick film element is 200–230 μm in thickness.

Results and Discussion

XRD Analysis

Following the successive flame spray procedures, the original powdered Ni–Cr–Fe alloy was converted into a thick film containing a mixture of metallic and oxide phases. To help identify the phases formed during this process, XRD analysis was used to examine the powder prior to heat treatment, after heat treatment and after deposition on a substrate. Diffraction patterns obtained from the alloy powder indicated that the material has the single-phase fcc structure predicted by the Ni–Cr–Fe ternary phase diagram [2]. The measured lattice parameter of 3.56 Å was consistent with values reported for the Inconel 600 parent material [3].

After the gas-atomised alloy had experienced its first flame spray heat treatment, a number of additional phases became detectable by XRD. A comparison with standard X-ray data files indicated that the processed powder contained a high



Fig. 1 Thick film electric heating elements deposited on the outside of a vacuum component

percentage of NiO, along with smaller quantities of Ni, the original alloy and a spinel (see Fig. 2). The flame spray deposition of this partially oxidised powder made no detectable difference to the phases present; however, the increased intensity of some of the diffraction peaks did indicate the preferential deposition of metallic phases. This difference between the metal and oxide deposition rates may be attributed to the disparity in the materials' melting temperatures. As the metallic phases soften at significantly lower temperatures than the oxide phases, a higher proportion of metal reaches a molten or semi-molten state, enabling it to bond more efficiently with the contact surface.

SEM/EDS Analysis of the Thick Film

The $\sim 200\text{-}\mu\text{m}$ -thick film, produced by flame spray deposition of the partially oxidised powder, consists of metallic particles embedded within an oxide matrix. Backscattered electron (BSE) imaging, of a specimen cross-sectioned parallel to the spray direction (see Fig. 3a), highlights the irregular distribution of the metallic phases amongst the lower atomic numbered oxides. The variation in the morphology of the metallic regions reflects the range of temperatures and velocities at which the material was deposited.

While the XRD results indicated that the majority of the film is NiO, EDS measurements acquired from regions of the bulk oxide $\sim 2\text{ }\mu\text{m}$ in diameter suggest the presence of significant quantities of Fe and Cr (see Fig. 3b, c). The most likely explanation for this is the incorporation of Fe and Cr into the NiO lattice structure during the powdered alloy's oxidation. Since Fe and Cr have similar ionic radii to Ni [4], they may replace Ni ions in the oxide lattice without significantly altering the lattice parameter.

The pseudo-binary Ni–Fe–O and Ni–Cr–O phase diagrams, published by Raghavan [5] and Kjellqvist [6], respectively, suggest that NiO can integrate appreciable quantities of Fe and Cr at high temperatures (such as those achieved during the oxidation treatment). As the oxidised material undergoes rapid cooling due to the water quench, this metastable high-temperature state may be maintained at room temperature where kinetics limit phase transformation. The limited effect of Fe and Cr dopants on the NiO lattice parameter has been reported elsewhere within

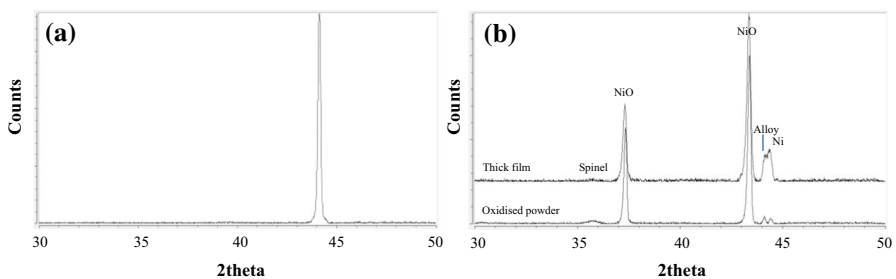


Fig. 2 XRD spectra from **a** gas-atomised powder and **b** a comparison of powder after oxidation and after consolidation into a thick film

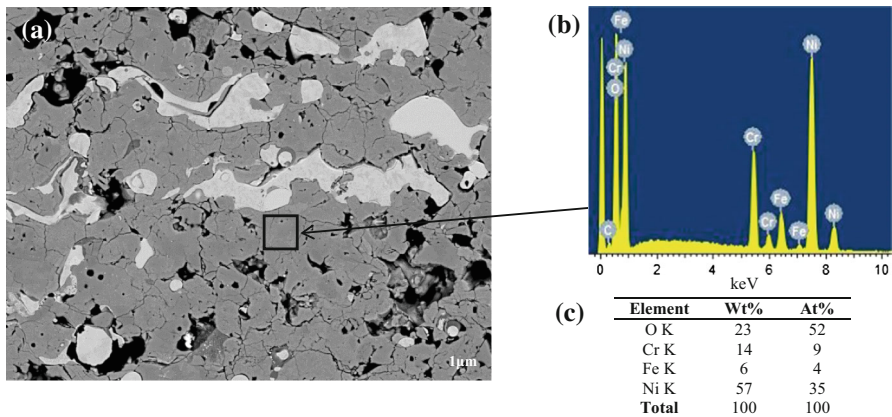


Fig. 3 **a** BSE image of a cross section through a thick film produced by spray deposition. The *light* regions are metallic phases, while the *grey* regions are oxide. Voids appear *black*. **b** An EDS spectrum from the oxide and **c** the corresponding quantitative analysis

the literature. Mallick et al. [7], who prepared Fe-doped NiO by chemical co-precipitation, found that the lattice parameter remained almost unchanged up to 3 at% Fe, before showing a slight increase at 5 at% Fe, while Elumalai et al. [8], who produced NiO doped with 1.5 at% Cr by the thermal decomposition of nitrates, measured a minor 0.3% decrease in the lattice parameter.

Depending upon the deposition conditions, material of similar chemical composition exhibited distinct differences in microstructure. As shown in Fig. 4a, b, the Cr- and Fe-doped NiO was present in both columnar and equiaxed grain structures. The columnar grain growth, orientated roughly parallel to the substrate surface, is a good indicator that some doped NiO is arriving at the surface in a molten state. Formation of these grains arises from heterogeneous nucleation at splat interfaces, followed by the rapid growth of crystals with fast growth directions orientated parallel to the direction of heat flow [9]. Conversely, the larger micron scale equiaxed grains are grouped in round clusters, indicating much less deformation upon surface contact. This material would appear to have arrived in

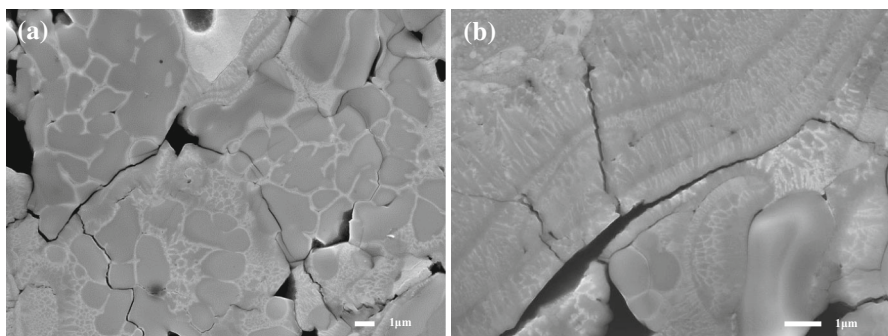


Fig. 4 Secondary electron images of **a** equiaxed and **b** columnar grains of doped nickel oxides

the solid state and retained some of the characteristics of the oxidised particle grain structure.

Combined XRD/SEM Analysis of Heat-Treated Thick Film

According to the pseudo-binary Ni–Fe–O and Ni–Cr–O phase diagrams, when a metastable Fe- and Cr-doped NiO is given the correct heat treatment, it should decompose to form more energetically favourable NiO plus spinel phases. In order to induce this response, a sample of the metal–metal oxide film was subjected to a 66-h heat treatment at 800 °C. The specimen was then examined using a combination of XRD and SEM.

XRD analysis of the film before and after heat treatment indicated that this decomposition was indeed occurring. Prior to heating, the spinel peaks were barely present in the diffraction pattern; however, following 66 h at 800 °C, the height of the spinel peaks increased appreciably (see Fig. 5).

SEM imaging also revealed a notable change in the microstructure of the oxidised material after heat treatment. As shown in Fig. 6, the interior of the doped NiO grains appeared homogeneous prior to heating. However, following 66 h at 800 °C, these oxidised regions developed a mottled appearance, suggesting the presence of two phases.

STEM Analysis of the Thick Film

To investigate the relationship between the spinel and doped NiO phases at high resolution, thin foil specimens were prepared using a FIB and analysed using a Jeol 2100 TEM/STEM. Samples were extracted from the thick film in its as-deposited state and after a 66-h heat treatment at 800 °C. Beginning with the as-deposited material, the distribution of the four main constituent elements within the doped NiO grains was assessed using EDS mapping. Within the interior of the grains, the Ni and O concentrations seemed to remain constant; however, the Cr and Fe appeared less evenly distributed with Cr concentrated in the centre of these grains, and Fe accumulated closer to the grain boundaries.

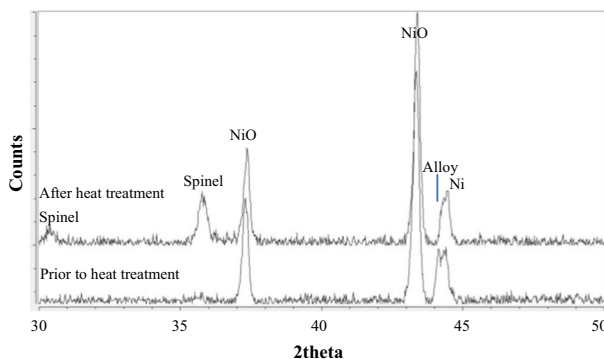


Fig. 5 XRD spectra from thick film heating elements before and after heat treatment at 800 °C for 66 h

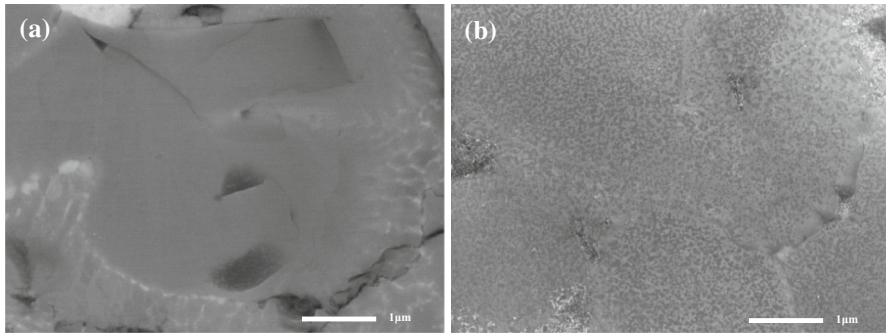


Fig. 6 Secondary electron images of doped nickel oxide grains **a** before and **b** after heat treatment

This effect may be related to Fe reducing the NiO melting temperature further than Cr [5, 6]. Small fluctuations in the composition of the liquid mixture cause localised differences in the element concentration. When the molten material cools, regions containing the highest concentrations of Cr solidify first, enriching the remaining liquid with Fe. This results in Cr and Fe concentrating in the interior and exterior of the grains, respectively, and the arrangement is preserved during rapid cooling of the sample to room temperature.

In addition to the composition variations within the doped NiO grains, the elemental mapping also detected the presence of grain boundary particles, primarily metallic nickel. The formation of these features may be attributed to Cr and Fe having a greater affinity for O than Ni [10]. When the molten mixture cools, the Cr and Fe react preferentially with oxygen, and in an oxygen-deficient atmosphere, the excess nickel is left as metallic particles at the oxide grain boundaries as shown in Fig. 7.

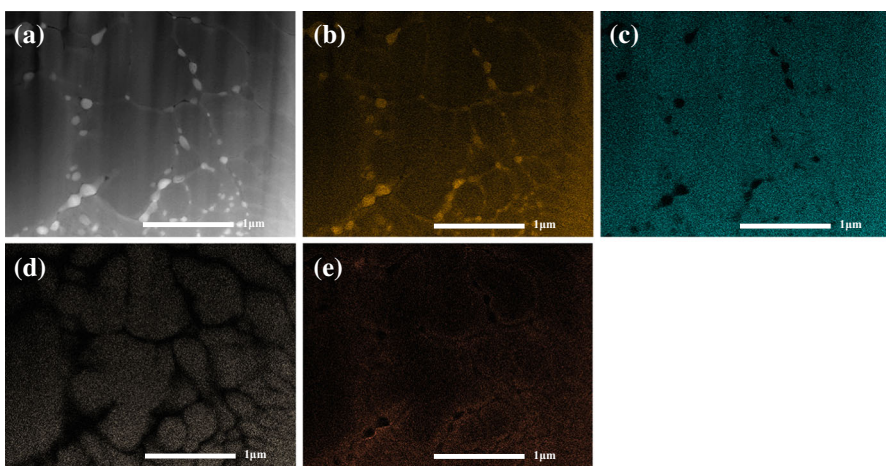


Fig. 7 **a** Secondary electron image and elemental EDS maps for **b** nickel, **c** oxygen, **d** chromium and **e** iron

When the material was examined at higher magnifications, variations between the oxide grains also became evident. In some grains, high-resolution imaging revealed a homogenous single-phase structure, as displayed in Fig. 8a. d-spacings calculated from these images, using FFT image analysis, proved consistent with the NiO values previously calculated from the XRD data. In contrast to this single-phase structure, other grains were found to contain arrays of approximately octahedral particles (Fig. 8b). FFT image analysis confirmed the d-spacings to be in agreement with the spinel and NiO values previously obtained through XRD.

FFT image analysis of these micrographs also helps highlight the close relationship that exists between the two structures. As the NiO matrix and the spinel particle are examined in turn, an additional set of diffraction spots appear at half intervals between the NiO spots. These correspond to the spinel 220 d-spacing that is approximately twice that of the 220 NiO d-spacing. The high degree of coherency between the NiO and spinel suggests that the oxygen sublattice is common to both structures and only the cations need to order for spinel precipitates to grow. This close coherency between NiO and spinel precipitates has previously been reported in both Fe-doped NiO [11] and Cr-doped NiO [12], with reported lattice misfits of <math><0.5\%</math>.

The variation in composition between the particles and the matrix was confirmed using EDS line scans. One example is displayed in Fig. 9, where the scan path (represented by a green line) can be seen intersecting two precipitates (appearing dark in the image). As the line scan passes over the particles, the Cr and Fe intensities peak, while the Ni dips and the O remains largely constant.

Thin foil specimens were also prepared from the heat-treated films (66 h at 800 °C). In contrast to the as-deposited films, the heat-treated specimens displayed evidence of spinel growth in all the doped NiO grains. The spinel particles were

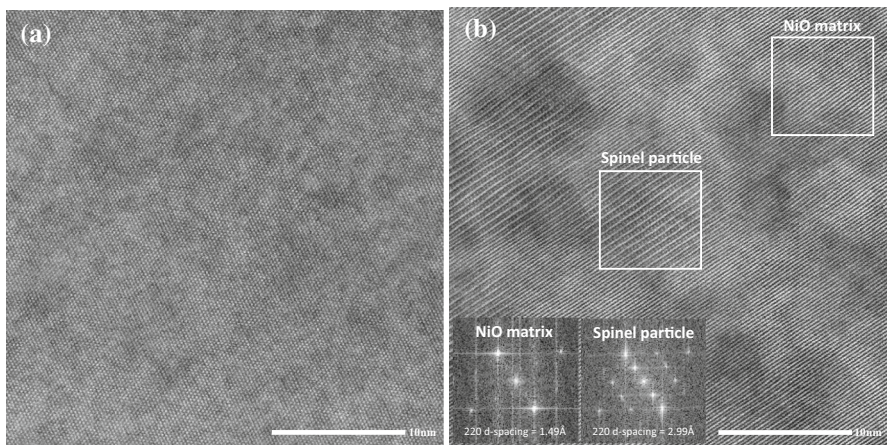


Fig. 8 High-resolution HAADF STEM images of **a** homogeneous doped single-phase NiO grains and **b** a NiO matrix containing spinel particles

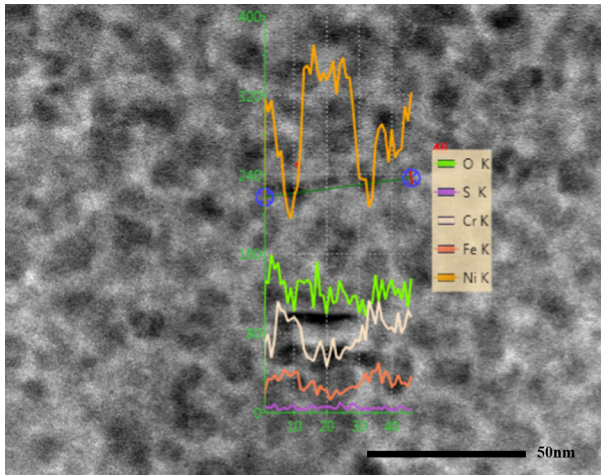


Fig. 9 Two-phase oxide region with elemental line scans between the *blue circles* (Color figure online)

larger—typically 40 nm in diameter as opposed to 20 nm before heat treatment—and were of similar size at both grain boundaries and within grains. Hence, homogeneous nucleation would appear to be relatively easy in this system. Once again, the characteristic double-layered superlattice structure of the spinel was distinguishable from the NiO matrix (see Fig. 10).

Further work is now underway to determine the precise composition and type of the particles (spinel or inverse spinel), using high-resolution STEM analysis to measure the site occupancy. However, this will form the basis of further paper.

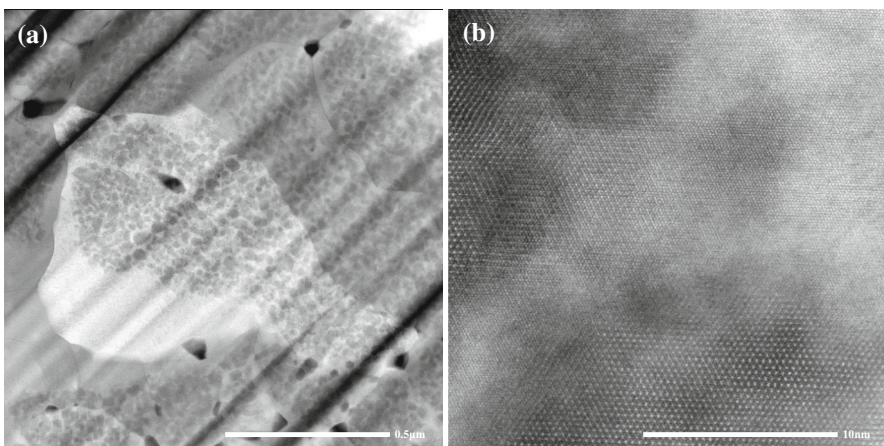


Fig. 10 HAADF STEM images of a FIB slice through a doped NiO sample after heat treatment at **a** low magnification and **b** high magnification, in which the extent of the spinel particles can clearly be observed

Conclusions

In a two-stage manufacturing procedure, flame spray technology was employed to produce novel metal–metal oxide thick films from a Ni–Cr–Fe powdered alloy. A combined SEM–EDS and XRD investigation of the deposited material identified the main consistent phases as alloyed metals, pure Ni, a spinel and an Fe- and Cr-doped NiO. In accordance with the pseudo-binary Ni–Fe–O and Ni–Cr–O phase diagrams, this doped NiO was observed to decompose to more energetically favourable NiO and spinel phases upon heat treatment at 800 °C. Spinel precipitation was further studied at high resolution, using TEM/STEM. In a thin foil TEM specimen cut from the as-deposited material, spinel growth was discovered intermittently across different NiO grains. However, following a 66-h heat treatment at 800 °C, spinel precipitation became evident across all the doped NiO grains. The spinel lattice parameter, calculated using FFT image analysis, was approximately twice that of the NiO matrix. Similar sized precipitates were observed within oxide grains and at grain boundaries, suggesting that homogeneous nucleation occurred easily throughout the oxide.

Acknowledgements The authors gratefully acknowledge the funding provided by the European Regional Development Fund through the Centre for Global Eco-Innovation.

Open Access This article is distributed under the terms of the Creative Commons Attribution 4.0 International License (<http://creativecommons.org/licenses/by/4.0/>), which permits unrestricted use, distribution, and reproduction in any medium, provided you give appropriate credit to the original author(s) and the source, provide a link to the Creative Commons license, and indicate if changes were made.

References

1. [http://www.specialmetals.com/documents/Inconel%20alloy%20600%20\(Sept%202008\).pdf](http://www.specialmetals.com/documents/Inconel%20alloy%20600%20(Sept%202008).pdf). Accessed 24 March 2015.
2. D. R. F. West and N. Saunders, *Selected Case Studies of Ternary Systems*, (Maney Publishing, London, 2002), pp. 129–136.
3. S. Raju, K. Sivasubramanian, R. Divakar, G. Panneerselvam, A. Banerjee, E. Mohandas and M. P. Antony, *Journal of Nuclear Materials* **325**, 2003 (18–25).
4. R. D. Shannon, *Acta Crystallographica* **A32**, 1976 (751).
5. V. Raghavan, *Journal of Phase Equilibria and Diffusion* **31**, 2010 (369–371).
6. L. Kjellqvist, M. Selleby and B. Sundman, *Computer Coupling of Phase Diagrams and Thermochemistry* **32**, 2008 (577–592).
7. P. Mallick, C. Rath, R. Biswal and N. C. Mishra, *Indian Journal of Physics* **83**, 2009 (517–523).
8. P. Elumalai, J. Zosel, U. Guth and N. Miura, *Ionics* **15**, 2009 (405–411).
9. R. McPherson, *Journal of Materials Science* **15**, 1980 (3141–3149).
10. R. Molins, B. Normand, G. Rannou, B. Hannoyer and H. Liao, *Materials Science and Engineering A* **351**, 2003 (325–333).
11. S. R. Summerfelt and C. B. Carter, *Philosophical Magazine A* **65**, 1992 (1503–1519).
12. C.-H. Chen, M. R. Notis and D. B. Williams, *Journal of the American Ceramic Society* **66**, 1983 (566–571).